Research Article

Hacettepe University Journal of the Faculty of Pharmacy
Volume 45 / Number 1 / March 2025 / pp. 57-70

Inhalable Pyrazinamide Loaded Lipid Polymer Hybrid Nanoparticles: *In-Vitro* and *In-Vivo* Lung Deposition Studies

Komal PARMAR[1]*
ORCID: 0000-0001-8564-163X
Urvi MAV[1]
ORCID: 0009-0008-1202-4057

[1]ROFEL Shri G.M. Bilakhia College of Pharmacy, Vapi, India

Corresponding author:
Komal PARMAR
ROFEL Shri G. M. Bilakhia College of Pharmacy, Rajju Shroff ROFEL University
E-mail: komal.parmar2385@gmail.com
Tel: +919714037405

Received Date: 14.10.2024
Accepted Date: 25.02.2025

DOI: 10.52794/hujpharm.1566707

ABSTRACT

In the present report, a nanoparticle based inhalable formulation of Pyrazinamide was prepared and evaluated for targeted drug delivery for pulmonary tuberculosis. Lipid polymer hybrid nanoparticles (LPHNs) loaded with pyrazinamide was prepared using emulsion-solvent evaporation technique with further optimization using design of experiments. Amount of polymer and lipid were chosen as the independent factors and particle size, percentage entrapment efficiency, and drug release at 6 hours (D6) were chosen as dependent variables. Optimized batch revealed particle size of 160.9 nm, % entrapment efficiency of 62.34 %, zeta potential of -27.45 mV and *in-vitro* drug release at 6 h of 75.18 %. The mean aerodynamic diameter of the particles was 0.845 µm which indicates ability to penetrate deep into the lungs. *İn-vivo* deposition studies demonstrated enhanced efficacy of the nano-formulation as compared to pure drug. Stability testing was expedited for the optimized batch of LPHN and the results confirmed no remarkable deviations in the values. Overall, the findings indicate LPHNs made of biodegradable lipid as a viable method for pulmonary drug administration of pyrazinamide.

Keywords: Pyrazinamide, LPHNs, Pulmonary drug delivery, Central composite design

1. Introduction

It is reported that about 2 billion of people in the world are suffering from pulmonary tuberculosis [1]. The *Mycobacterium tuberculosis* (*M. tuberculosis*) infects macrophages, which complicates the tuberculosis drug therapy procedure. Many antibacterial treatments are effective in preventing *M. tuberculosis*, but they also come with unavoidable problems, chief among them being drug resistance [2,3]. Numerous cutting-edge drug-delivery methods have been studied in an effort to boost therapeutic efficacy, decrease adverse effects, and enhance patient compliance. The nano-based drug delivery overcomes the antiquated methods of the standard anti-tubercular regimen. Consequently, nanoparticle-based technology has shown convincing therapies and encouraging outcomes for long-term infectious diseases like tuberculosis [4-7]. Various investigators have demonstrated inhalable nanoparticles such as spray dried effervescent nanoparticles [8], polymeric nanoparticles [9, 10], solid lipid nanoparticles [11] for successful targeted drug delivery for the management of pulmonary tuberculosis.

Liposomes are specially designed vesicles that disperse synthetic or natural amphipathic lipids in water to spontaneously form one or more bilayers. But when it comes to poorly water soluble drugs, liposomes have poor encapsulation efficiency specifically with small unilamellar vesicle type of liposomes [12]. Synthetic or semi-synthetic biodegradable polymers are used to create polymeric nanoparticles, which are colloidal particles encasing the drug [13]. Lipid-polymer hybrid nanoparticles, or LPHNs, represent a new method in nano-based medication delivery for the management of many long-lasting illnesses [14-16]. For example, in non-alcoholic fatty liver disease, Liang and colleagues produced chitosan functionalized LPHNS for silymarin oral administration and improved the cholesterol lowering efficacy [17]. Another study effectively developed LPHNs laden with docetaxel to target cells of metastatic prostate cancer [18]. Liposomes and polymeric nanoparticles share conceptual similarities with LPHNs, which consist of a polymer core encased in a lipid layer. LPHNs combine the advantages of both the systems and offer extended systemic circulation, high drug loading, biocompatibility, stability, and controlled release capability [19- 21].

Pyrazinamide is indicated primarily for tuberculosis treatment [22]. Pyrazinamide is significantly more efficient than other antibiotics. However, it has less efficiency against latent resilient bacterial strains [23]. In the acidic pH produced by bacteria, Pyrazinoic acid, an active form is formed from Pyrazinamide. İn acidic pH of bacteria, pyrazinamide changes into its active moiety, pyrazinoic acid, which further impede the growth and replication-related enzyme fatty acid syntheses I [24]. The major side effect of dose-dependent pyrazinamide is hepatotoxicity, along with nausea, vomiting, loss of appetite, or mild muscle/joint pain [25]. Resistance to pyrazinamide in *Mycobacterium tuberculosis* is also reported [26]. İn recent studies, various investigators have demonstrated inhalable nanoparticles for the delivery of pyrazinamide for the treatment of pulmonary tuberculosis [27-29].

The active moeity of pyrazinamide is lipophilic in nature. The lipid core maintains high encapsulation for lipophilic drugs, while the polymeric shell increases the stability of the nanoparticles and protects the drug during blood circulation against external factors [30, 31]. Thus, the goal of the research is to produce an oral dry powder drug delivery system for lipid polymer hybrid nanoparticles loaded with pyrazinamide. This will overcome the drawbacks of using traditional oral dosage forms of pyrazinamide and individual types of nanoparticles (lipid or polymeric) by combining the benefits of liposomes and polymeric nanoparticles separately in the formulation and delivering direct drug delivery to the target organ. The process and formulation factors were optimised through the use of central composite design. The prepared nanoparticles were assessed for various parameters.

2. Material and Methods

2.1. Materials

Pyrazinamide was obtained as gift sample from Macleods Pharma Ltd., Ankleshwar, India. Soya lecithin was purchased from Vishal Chemicals, Mumbai, India. Isopropyl myristate was obtained from High Purity Laboratory Chemicals, Mumbai, India. Oleic acid was procured from Clairo Filt, Mumbai, India. HPMC E15 was obtained from The Dow Chemical Co., Bangalore, India. Span 80, Poly vinyl alcohol and Lactose Monohydrate was obtained from Ozone

International, Mumbai, India. Dichloromethane and Methanol was procured from Thomas Baker, Mumbai, India.

2.2. Methods

2.2.1. Preparation of Pyrazinamide loaded LPHN

LPHNs of pyrazinamide were fabricated by emulsification-solvent evaporation technique [32]. Briefly, a mixture of; lipid and polymer dissolved in dichloromethane (3 ml) and drug dissolved in methanol (2 ml) was prepared. Further, the oil phase was added gradually into the solution (30 ml) consisting of 1%w/v surfactant (Span 80) in water under the high-speed stirring (10000 rpm). Continuous stirring of the mixture was carried out for specific period of time. Then the mixture was further sonicated for 15 min using Ultrasonic bath (EIE Instruments, Ahmedabad, India) and spray dried using spray dryer (LSD-48, JISL, Mumbai, India) to obtain powder nanoparticles.

2.2.2. Scrutinization of variables

Various formulation and process variables were scrutinized for further optimization. Three different lipids namely soya lecithin, isopropyl myristate and oleic acid were taken in Eppendorf tube. Surplus amount of drug around 500 mg was added in the lipid (3 ml) and exposed to shaking at 25□ using orbital incubator shaker (EIE Instruments, Ahmedabad, India) for a period of 48 h. Later, the dispersion was centrifuged at 10000 rpm for 10 min. Supernatant was appropriately diluted with methanol and analyzed using UV-Visible Spectrophotometer (Shimadzu 1800, Japan) at 263 nm. Further, concentration of lipid was varied from 50 to 250 mg to check the effect of variation on particle size and entrapment efficiency (EE) of the LPHNs. Then, nanoparticles were prepared at different stirring time at 24, 28 and 32 h to assess the influence of stirring time on the formation of LPHNs. Different concentration of HPMC E15 (polymer) varying from 50 to 250 mg were taken while keeping all other parameters constant. Table 1 summarizes the formulation details of the preliminary trial batches. Further, prepared LPHNs were analyzed for particle size and EE.

2.2.3. Optimization using central composite design

The process of developing a pharmaceutical formulation takes a long time and requires changing one variable at a time through trial and error. From the preliminary studies, two independent variables were identified influencing the formation of the nanoparticles. Central composite design (CCD) presents a notable benefit over factorial design due to its proficiency in modeling nonlinear relationships and curvature in a response surface. The addition of center and axial points allows for a more extensive analysis of quadratic effects, often resulting in a reduced number of experimental runs when compared to a full factorial design. Two factor-three level central composite design was used in this study to determine how independent and dependent variables interacted [33,34]. Table 2 demonstrates values of independent variables shown in coded and actual form. Dependent responses for optimization taken were Particle size (nm) (Y_1), % Entrapment Efficiency (Y_2) and % Drug release at 6 h (D6) (Y_3). ANOVA and multiple regression analysis were examined to determine the implemented model's statistical significance and impact. Design Expert 10.0 was used to build the nonlinear quadratic model. R^2 values and the statistically significant co-efficient were used to assess the implemented model. Using the overlay plot and the chosen criteria, the optimized batch was produced and evaluated. The % relative error was computed by quantitatively comparing the experimental values obtained from the responses with the theoretical value.

2.2.4. Particle size, PDI and Zeta potential analysis

Particle size, PDI, and zeta potential of produced batches of Pyrazinamide LPHNs were measured using a Malvern Zetasizer. A batch of LPHNs that had been optimized was diluted 100 times and used in the study.

2.2.5. % Entrapment efficiency (EE)

The 50 mg of sample was appropriately washed with methanol to remove any free drug. They were then dried, further triturate with methanol and sonicated for 15 mins to release the encapsulated drug. It was then filtered, and the solutions were analysed spectrophotometrically at 263 nm. Standard formulas were used to calculate the encapsulation efficiency.

2.2.6. Drug release analysis and release kinetics

The release studies was performed using dissolution test apparatus II (Paddle type, LabIndia, India). The rotation of the paddles was 100 rpm, and the temperature was maintained at 37°C ± 0.5°C. Briefly,

ISSN: 2458 - 8806

Table 1. Formulation of preliminary trial batches

Batch code	Trial Variable	Constant
	Concentration of Lipid (mg) (Soya Lecithin)	Amount of drug (10 mg), Amount of polymer (100 mg), stirring time (28 h) and stirring speed (10000 rpm)
S1	50	
S2	100	
S3	150	
S4	200	
S5	250	
	Stirring time (h)	Amount of drug (10 mg), Amount of polymer (100 mg), Amount of Lipid (100 mg) and stirring speed (10000 rpm)
T1	24	
T2	28	
T3	32	
	Concentration of Polymer HPMC E15 (mg)	Amount of drug (10 mg), Amount of Lipid (100 mg), stirring time (28 h) and stirring speed (10000 rpm)
P1	50	
P2	100	
P3	150	
P4	200	
P5	250	

Table 2. Independent variables with coded and actual values

Translation of coded value in actual units			
Independent variables	**Variable levels**		
	Low (-1)	**Medium (0)**	**High (+1)**
Concentration of polymer (mg) (X_1)	100	150	200
Concentration of lipid (mg) (X_2)	100	150	200

LPHNs consisting of 50 mg of pyrazinamide were taken in the dialysis bag. The dialysis bag was tied to a paddle and dipped in the phosphate buffer, pH 7.4 [35]. Then, 5 mL samples were withdrawn after specific periods and replenished with an equal volume of new media. Spectrophotometric analysis was performed on the filtered samples. The release studies were performed in triplicate, and the average values as cumulative percent drug released versus time was plotted. The release of the drugs from the sample was analyzed using a variety of kinetic models. Based on the regression coefficient (R^2), the most ap-

propriate model for defining the release mechanism was selected [36].

2.2.7. Fourier Transform Infrared Spectroscopy (FT-IR)

FTIR spectrophotometer was recorded for pure drug and optimized sample (Shimadzu, Japan). Each spectrum was recorded with a sensitivity of 4 cm^{-1} in a dry atmosphere to avoid filthy contributions and averaged over 100 repetitions, resulting in a good signal-to-noise ratio and reproducibility and scanned between the 4000-450 cm^{-1} range.

2.2.8. Scanning electron microscopy (SEM)

Field Emission SEM (JSM-7610F Plus, JEOL) was used to determine the surface morphology of optimized sample. Using a double-sided carbon adhesive tape, the nanoparticles were frivolously scattered on the tape. Those were then impacted on gold-coated aluminium stubs of 300 Å to reduce the charging effects and photomicrographs were taken at an accelerating voltage of 20 kV.

2.2.9. Micromeritics

To determine the flow characteristics of the batch of polymeric nanoparticles that was optimized, the angle of repose and Hausner's ratio were calculated. Using a fixed funnel approach and a fixed height of 2 cm, the angle of repose was measured. Standard equations were used to obtain angle of repose and Hausner's ratio values.

2.2.10. In-vitro deposition studies

The optimized batch's mean median aerodynamic diameter was computed using an Anderson eight-stage cascade impactor (Mumbai, India) [37]. Using HPLC analysis, the pyrazinamide content was determined at each stage after LPHNs of the compound were passed through a cascade impactor at a rate of 28.3 l/min. The mobile phase consisted of 2% v/v acetonitrile in a pH 4 potassium phosphate buffer (5 mM). The flow rate was 1 ml/min. MMAD and geometric standard deviation were obtained using MMADCALCULATOR [38].

2.2.11. In-vivo deposition studies

In-vivo deposition studies were carried out using two groups of six rats each (Protocol sanction ID: ROFEL/IAEC/2021/0015). Wistar rats of any sex weighing 200-250 g were taken for the study. The animals were subjected to appropriate conditions of light and feed for 24 h before the starting the study. One group of rats was feed with optimized formulation of nanoparticles and the other group with pure drug powder. Administration of both samples were carried out using method reported wherein the syringe was filled with powder sample and placed near the nostrils of the rats via 20 G cannula tube. Later the rats were sacrificed for deposition analysis in the pulmonary region wherein the lungs were isolated and sections were studied under light microscopy for the deposition of nanoparticles in the tissue. Also, trachea and lungs were blended with phosphate buffer solution (15 ml). The blend was treated with trichloroacetic acid for deproteination and sodium bicarbonate for neutralization of acid. The sample was then centrifuged at 150000 rpm for 5 min and supernatant was subjected for analysis of drug amount by HPLC method.

2.2.12. Accelerated Stability Study

Optimized batch of LPHNs was subjected to accelerated stability testing using a stability chamber. Sample powder was sealed in aluminum container and stabilized for 6 months at 40ºC/75% RH. Particle size, zeta potential, drug content, and *in-vitro* drug release were assessed for samples every 3 months till 6 months.

3. Results and Discussion

3.1. Preliminary trial studies

Screening was carried out to determine the influence of formulation and process variables on the generation of pyrazinamide lipophilic nanoparticles (LPHNs). Solubility tests were used to examine lipids, and the results displayed in Figure 1 indicated that soy lecithin had the maximum solubility of pyrazinamide, which was then used for additional optimization. Further, different concentration of soya lecithin was assessed while keeping all other parameters constant (Table 3). The results of the variation in lipid concentration, as displayed in Table 3, showed that the particle size increased as lipid content increased. This might be attributed to more amount of lipid content available to get adsorb on the surface of the particles [39]. Furthermore, the increased molecular weight of solid lipids may serve as an additional factor, poten-

ISSN: 2458 - 8806

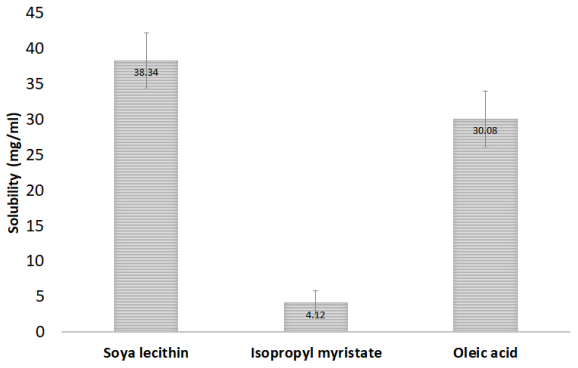

Figure 1. Solubility of pyrazinamide in different lipids

Table 3. Preliminary trials for screening of variables

Screening	Batches	Particle size (nm)
Concentration of lipid (Soya lecithin)	S1	209.5 ± 4.67
	S2	135.7 ± 2.24
	S3	159.9 ± 2.98
	S4	175.5 ± 3.01
	S5	179.5 ± 3.33
Stirring time (h)	T1	257.5 ± 3.96
	T2	135.7 ± 2.51
	T3	132.3 ± 2.19
Concentration of polymer (mg) (HPMC E15)	P1	246.4 ± 3.25
	P2	135.7 ± 2.63
	P3	169.7 ± 2.88
	P4	186.2 ± 3.05
	P5	201.2 ± 2.84

tially leading to more intricate linkages among the molecules. This complexity could ultimately result in aggregation, which may contribute to an increase in particle size [40]. However, particle size was also observed to be greater when lipid content was lower, which may be related to drug precipitation from the lipid [41]. Further, stirring time was screened for 24, 28 and 32 h, and the results showed no apparent variation in LPHN particle size. This implies that the particles might have reached to the stable state where further stirring does not remarkably affect the particle size. HPMC E15 was taken as the polymer for the preparation of lipid polymer hybrid nanoparticles of pyrazinamide. Screening of amount of polymer was done to check the influence of varying the amount on the formation of LPHNs. Results exhibited rise in particle size with rise in polymer quantity [42]. The probable cause of this might be attributed to the increasing viscosity of the dispersed phase, leading to a decreased dispersibility of the polymer solution in the aqueous phase. As the polymer concentration rises, the viscous forces resist the breakdown of the particles [43-45]. The initial batch, however, displayed a higher side of particle size, which may indicate that there was less polymer available to reduce the size of the drug particles.

3.2. Optimization using Central Composite Design

Optimal batches of LPHNs were obtained by applying the Central Composite Design. Particle size, % EE, and % drug release were chosen as optimization factors for the prepared design batches. Particle size of the nanoparticles gives the idea of the formation of particles in the nanometer range. %EE of the nanoparticles gives the idea of the amount of drug entrapped in the formed nanoparticles and % drug release gives the idea of the drug release pattern from the nanoparticles. These parameters are important to assess the performance of the nanoparticulate drug delivery. Table 4 tabulated the responses of design batches. It was observed that responses of all 9 batches concurrently fitted to quadratic model with R^2 values for Y_1(0.9725), Y_2(0.9470), and Y_3(0.9932) employing Design Expert Version 10. Quadratic equations found from the process are as follows:

$$Y_1 = +175.46+17.55X_1+10.68X_2-6.95X_1X_2- 0.48X_1^2 -0.58X_2^2 \text{ -eq 1}$$

$$Y_2 = +70.12+0.02X_1+2.73X_2-4.84X_1X_2-4.04X_1^2 - 3.22X_2^2 \text{ -eq 2}$$

$$Y_3 = +69.14-3.98X_1-4.29X_2+2.09\ X_1X_2-1.09\ X_1^2 - 0.12X_2^2 \text{ -eq 3}$$

The findings of particle size responses indicated that the independent factors (X_1 and X_2) chosen for the analysis had a positive impact on particle size (Y_1). Specifically, an increase in the values of X_1 and X_2 indicated a bigger particle size. The observed increase in particle size may be attributed to the rising viscosity of the solution, which subsequently led to an enhancement in the liquid phase resistance of the particle dispersion. As a result, the particle size can be augmented by fostering greater interconnection among the particles. Thus, by elevating the number of particles, the rate of interconnection between them was enhanced, culminating in the formation of larger nanoparticles [46]. These two variables X_1 and X_2 were found to be significant with P value less

Table 4. Responses of design batches

Batch	Particle size (nm) (Y_1)	%EE (Y_2)	Drug release at 6 h (D6) (Y_3)
F1	135.7 ± 2.51	53.21 ± 1.56	78.02 ± 1.52
F2	186.2 ± 3.05	67.93 ± 1.76	66.53 ± 1.54
F3	175.5 ± 3.01	66.82 ± 1.59	65.32 ± 1.49
F4	198.2 ± 2.49	62.18 ± 1.47	62.19 ± 2.43
F5	159.9 ± 2.98	62.70 ± 1.41	72.52 ± 2.32
F6	192.0 ± 2.36	70.75 ± 1.63	63.24 ± 1.54
F7	169.7 ± 2.88	63.29 ± 1.43	73.19 ± 1.48
F8	182.0 ± 2.71	71.80 ± 1.65	64.52 ± 2.56
F9	173.5 ± 2.05	68.82 ± 1.57	69.47 ± 2.35

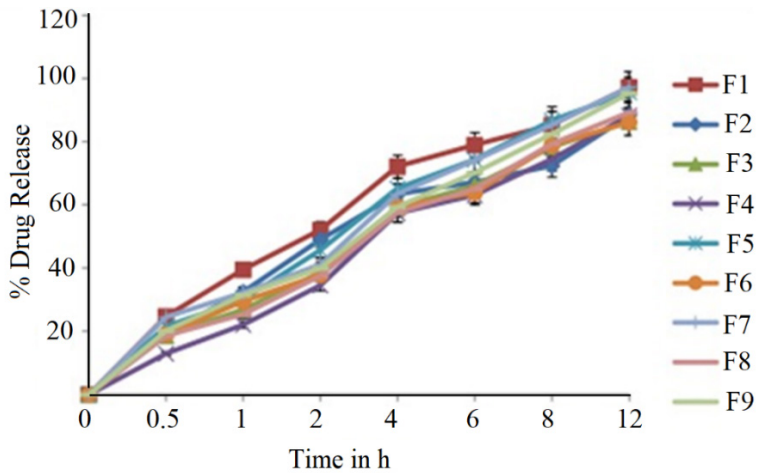

Figure 2. Dissolution profile of design batches

than 0.05 in influencing Y_1 whereas, the interaction effect X_1X_2 was found to be non-significant. The response value for %EE for all nine batches F1-F9 was found to be from 53.21 to 71.80%. Independent factors, the X_1 and X_2 had a positive impact on the dependent variable Y_2. Thus, drug entrapment efficiency was higher with increase in lipid and polymer amount. This might be due to larger cavity available in the nanoparticle, allowing more drug to be contained within the nanoparticle. Additionally, optimal amount of lipid and polymer contribute to the stability of the nanoparticles, thereby preventing the premature leakage of the drug [47, 48]. The individual variables X_1 and X_2 and interaction effect X_1X_2 were found to be significant with P value less than 0.05 in influencing Y_2 response. The observed responses for D6 for all nine batches F1-F9 varied from 62.19 to 78.02%. Figure 2 shows the drug release profile of all the design batches. The independent variables, X_1 and X_2 showed opposite influence with negative value of co-efficient. Lipids and polymers create a matrix surrounding the drug molecules, functioning as a barrier that hinders its movement and subsequent release [49]. The individual variables X_1 and X_2 and interaction effect X_1X_2 were found to be significant with P value less than 0.05 in influencing Y_3 response. The response surface non-linear quadratic model showed the best fit, with a P-value <0.05, according to the results (Table 5). Further, overlay plot (Figure 3) was produced using selection criteria for all responses, including 130-160 for particle size, 55-75 for % EE, 65-80 for D6. Table 6 shows that there was less than 5% percent relative error between the experimental and theoretical values. Desirability function value for the optimized batch was shown to be 0.86. When the responses have a desirability

ISSN: 2458 - 8806

Table 5. Results of ANOVA of dependent variables

Sources	Sum of square	Degree of freedom	Mean square	F-value	P-value
For Y_1= Particle size					
Regression	1075.34	5	215.06	31.15	0.0313
Residual	13.80	3	6.90		
Total	1089.15	8			
For Y_2 = %Entrapment Efficiency					
Regression	246.47	5	49.29	10.72	0.0390
Residual	13.78	3	4.59		
Total	260.26	8			
For Y_3= Drug release at 6 h (D6)					
Regression	225.37	9	45.07	87.67	0.0018
Residual	1.54	3	0.514		
Total	226.91	12			

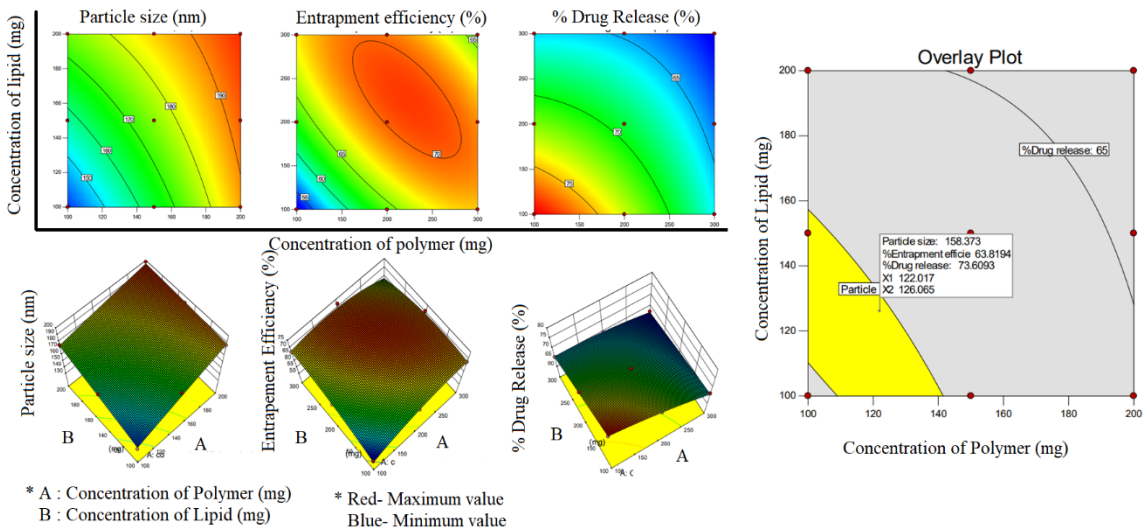

Figure 3. Graphs; Contour plots, 3d response graphs, and Overlay plot

Table 6. Result of optimized Batch for Response Variable

Response Variables	Optimized batch		
	Theoretical value	Practical value	% Relative error
Particle Size (nm)	158.37	160.9 ± 2.23	1.59
%EE	63.81	62.34 ± 1.54	2.30
D6	73.61	75.18 ± 2.36	2.13

value of 1, it indicates the most desired value; a value of 0 indicates an undesired value [50].

3.3. Fourier Transform Infrared Spectroscopy (FT-IR)

To investigate latent interactions between the drug and excipients in the prepared LPHNs, FT-IR analysis was conducted. Figure 4 displays the FTIR spectroscopy findings wherein the functional group peaks of pyrazinamide such as N-H stretching (3414.25 cm^{-1}), C-N stretching (1378.65 cm^{-1}), C=O stretching (1714.53 cm^{-1}) and C-H stretching (3160.37 cm^{-1}) were observed in the FT-IR graph of the optimized batch suggesting that there was no remarkable interaction between the drug and the polymers [51].

3.4. Scanning electron microscope (SEM)

The outcome of the electron microscopy of the optimized batch is displayed in Figure 5. The lipid-polymer matrix system's drug amalgamation and crystal structure were validated by SEM investigations. Figure demonstrated uniform dispersion of drug into the lipid-polymer matrix.

3.5. Micromeritic properties

Micromeritics characteristics of the best formulation of LPHNs were quantified. Value of angle of repose was found to be 21.33º ± 0.98 and that of Hausner's ratio was found to be 1.19 ± 0.15. The obtained results suggested acceptably good flow properties (Angle of repose < 25º and Hausner's ratio <1.19) of the powdered formulation [52].

3.6. Kinetic modelling

Calculating the coefficient of determination (R^2) is a common method to evaluate the suitability of model equations. The model with the highest adjusted (R^2) considered the best fit and is selected for further study. A (R^2) regression coefficient value close to 1 served as the basis for the interpretation of the kinetic drug release data [53]. The Higuchi model was found to be appropriate with an R^2 value of 0.993, which supports the diffusion mechanism. In contrast,

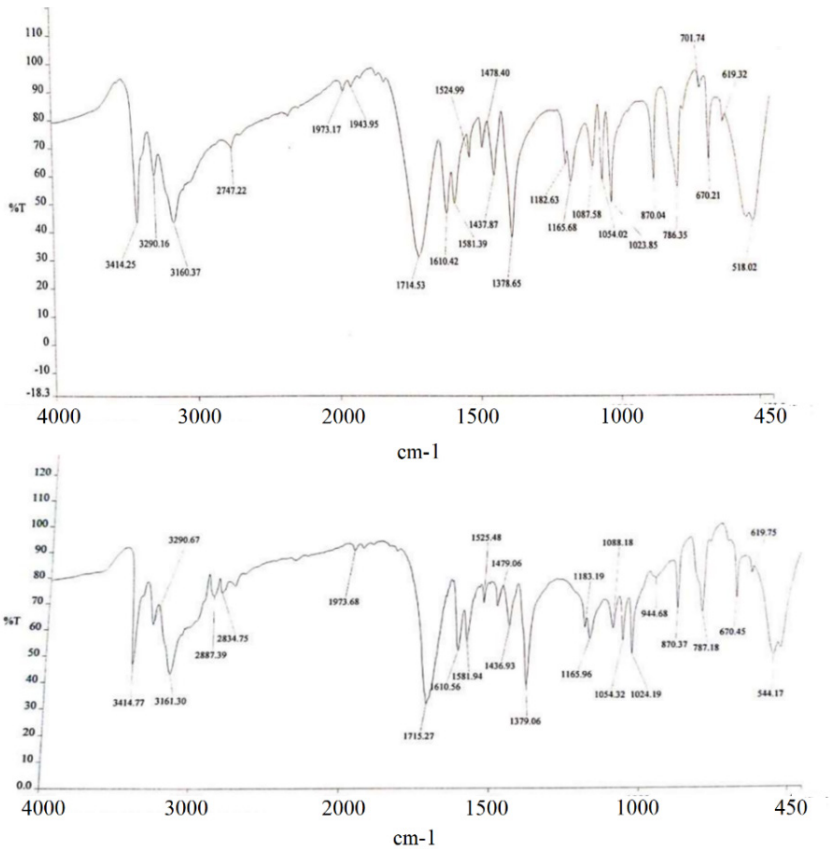

Figure 4. FT-IR Analysis of pure drug (a) and optimized LPHNs of pyrazinamide (b)

ISSN: 2458 - 8806

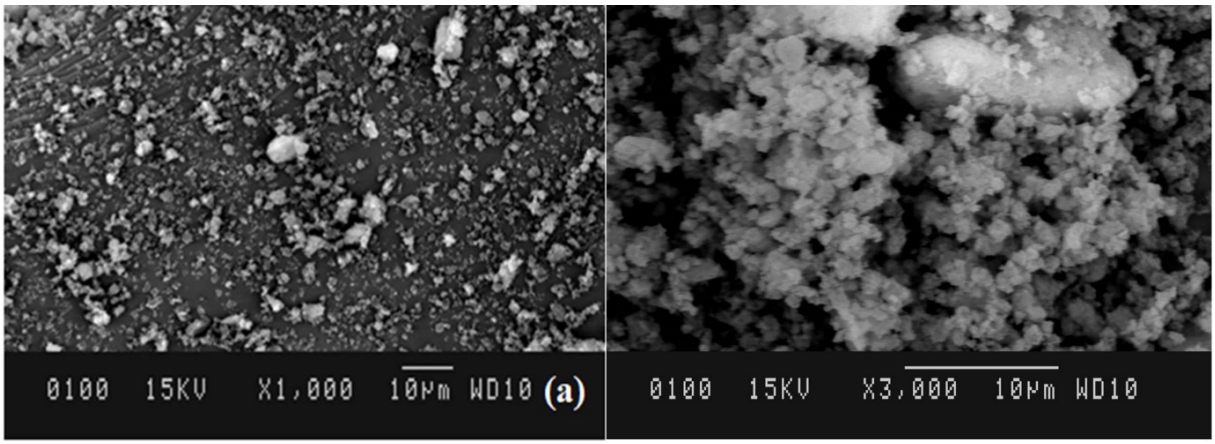

Figure 5. SEM Analysis of pure drug (a) and optimized LPHNs of pyrazinamide (b)

the R^2 values of the zero order, first order, Korsemeyer Peppas, and Hixson Crowell cube root models were 0.940, 0.545, 0.859, and 0.631, respectively.

3.7. In-vitro deposition studies

The shape and size of a particle are the key variables that influence its retention in varied lung areas. Particles with an aerodynamic size range of 0.5 to 5 µm can penetrate small airways and alveoli [54]. Optimized batch of LPHNs exhibited Aerodynamic particle size of 0.845 µm. Further, value of geometric standard deviation was found to be 0.91. The optimum value of particle size obtained in the MMAD analysis suggested deeper retention of the powdered formulation in the lungs.

3.8. In-vivo deposition studies

İn-vivo studies were carried out to check the deposition of the prepared nanoparticles in the pulmonary region. Histopathology studies revealed the uptake of nanoparticles in the lung tissue (Figure 6). İn addition, drug loaded nanoparticles were analysed for their deposition in the trachea and lungs. Results exhibited 1.21 and 2.66 times more drug deposition in trachea and lungs from the optimized batch of nanoparticles as compared to pure drug deposition in the respective regions. The smaller particles of the optimized batch facilitates the deeper deposition in the pulmonary system [55, 56]. The % uptake was statistically higher with $P < 0.05$ according to Student T-test.

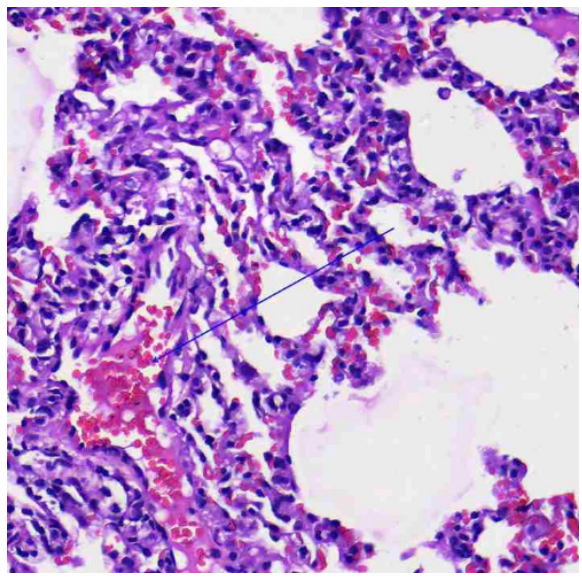

Figure 6. Histopathology of lung for nanoparticles deposition studies

3.9. Accelerated Stability Study

From the stability studies it was concluded that there was no remarkable change in the values of the parameters with P value less than 0.05, suggesting stability of the formulation for 6 months as a minimum (Table 7).

Table 7. Accelerated stability data of formulation

Parameter	Initial	After 3 month	After 6 month
Appearance	Creamy white powder	Creamy white powder	Creamy white powder
Drug content (%)	97.56 ± 0.78	98.08 ± 0.93	97.28 ± 0.75
% *In-vitro* drug release at 6h	75.18 ± 2.36	75.44 ± 1.46	75.42 ± 1.42
Particle size (nm)	160.9 ± 2.23	165.5 ± 2.47	163.3 ± 2.31
Zeta Potential (mV)	-27.45 ± 1.95	-27.59 ± 2.06	-28.53 ± 2.39

system and with appreciable entrapment efficiency. The drug release mechanism from the LPHNs was demonstrated by the release kinetics, which adhered to the Higuchi model. Particle aerodynamic diameter was within the range that the alveolar region could hold onto. Studies on accelerated stability revealed that nanoparticles were stable for at least six months.

Acknowledgements

Authors are grateful to Macleods Pharma Ltd., Ankleshwar, India for providing gift sample of drug for the research purpose.

Conflict of Interest

Authors declare that they do not have any conflict of interest with respect to the mentioned work publication.

Statement of Contribution of Researchers

Conceptualization, Data Analysis, Review and editing of the manuscript: K.P.; Practical work, data curation, manuscript preparation: U.M.

4. Conclusions

Pyrazinamide LPHNs were made by emulsification solvent evaporation method. In order to maximise the process and formulation variables, central composite design was utilized. The optimized batch had microscopic particles that could enter the pulmonary

References

1. Moutinho S. Tuberculosis is the oldest pandemic, and poverty makes it continue. Nature. 2022;605:S16-S20. https://doi.org/10.1038/d41586-022-01348-0.
2. Gygli SM, Borrell S, Trauner A, Gagneux S. Antimicrobial resistance in *Mycobacterium tuberculosis*: mechanistic and evolutionary perspectives. FEMS Microbiol Rev. 2017;41(3):354-73. https://doi.org/10.1093/femsre/fux011.
3. Singh R, Dwivedi SP, Gaharwar US, Meena R, Rajamani P, Prasad T. Recent updates on drug resistance in *Mycobacterium tuberculosis*. J Appl Microbiol. 2020;128(6):1547-67. https://doi.org/10.1111/jam.14478.
4. Machelart A, Salzano G, Li X, Demars A, Debrie AS, Menendez-Miranda M, et al. Intrinsic antibacterial activity of nanoparticles made of β-cyclodextrins potentiates their effect as drug nanocarriers against tuberculosis. ACS Nano. 2019;13:3992-4007. https://doi.org/10.1021/acsnano.8b07902.
5. Maretti E, Costantino L, Rustichelli C, Leo E, Croce MA, Buttini F, et al. Surface engineering of Solid Lipid Nanoparticle assemblies by methyl α-d-mannopyranoside for the active targeting to macrophages in anti-tuberculosis inhalation therapy. Int J Pharm. 2017;528(1-2):440-51. https://doi.org/10.1016/j.ijpharm.2017.06.045.
6. Poh W, Ab Rahman N, Ostrovski Y, Sznitman J, Pethe K, Loo SCJ. Active pulmonary targeting against tuberculosis (TB) via triple-encapsulation of Q203, bedaquiline and superparamagnetic iron oxides (SPIOs) in nanoparticle aggregates. Drug Deliv. 2019;26(1):1039-48. https://doi.org/10.1080/10717544.2019.1676841.

ISSN: 2458 - 8806

7. Ramalingam V, Sundaramahalingam S, Rajaram R. Size-dependent antimycobacterial activity of titanium oxide nanoparticles against: *Mycobacterium tuberculosis*. J Mater Chem B. 2019;7:4338-46. https://doi.org/10.1039/C9TB00784A.
8. Rai PY, Sansare VA, Warrier DU, Shinde UA. Formulation, characterization and evaluation of inhalable effervescent dry powder of Rifampicin nanoparticles. Indian J Tuberc. 2023;70(1):49-58. https://doi.org/10.1016/j.ijtb.2022.03.007.
9. Ivana Romina I R, Benjamín B, Melina Mara M M, Gladys Ester G E. Quantification of rifampicin loaded into inhaled polymeric nanoparticles by reversed phase high-performance liquid chromatography in pulmonary nonphagocytic cellular uptake. Anal Methods. 2024;16(13):1908-1915. https://doi.org/10.1039/d4ay00234b.
10. Mukhtar M, Csaba N, Robla S, Varela-Calviño R, Nagy A, Burian K, Kókai D, Ambrus R. Dry powder comprised of isoniazid-loaded nanoparticles of hyaluronic acid in conjugation with mannose-anchored chitosan for macrophage-targeted pulmonary administration in tuberculosis. Pharmaceutics. 2022;14(8):1543. https://doi.org/10.3390/pharmaceutics14081543.
11. Nemati E, Mokhtarzadeh A, Panahi-Azar V, Mohammadi A, Hamishehkar H, Mesgari-Abbasi M, et al. Ethambutol-loaded solid lipid nanoparticles as dry powder inhalable formulation for tuberculosis therapy. AAPS PharmSciTech. 2019;20(3):120. https://doi.org/10.1208/s12249-019-1334-y.
12. Gonzalez Gomez A, Hosseinidoust Z. Liposomes for antibiotic encapsulation and delivery. ACS Infect Dis. 2020;6(5):896-908. https://doi.org/10.1021/acsinfecdis.9b00357.
13. Zielińska A, Carreiró F, Oliveira AM, Neves A, Pires B, Venkatesh DN, et al. Polymeric nanoparticles: Production, characterization, toxicology and ecotoxicology. Molecules. 2020;25(16):3731. https://doi.org/10.3390/molecules25163731.
14. Bachhav SS, Dighe VD, Kotak D, Devarajan PV. Rifampicin Lipid-Polymer hybrid nanoparticles (LIPOMER) for enhanced Peyer's patch uptake. Int J Pharm. 2017;532(1):612-22. https://doi.org/10.1016/j.ijpharm.2017.09.040.
15. Tahir N, Madni A, Correia A, Rehman M, Balasubramanian V, Khan MM, et al. Lipid-polymer hybrid nanoparticles for controlled delivery of hydrophilic and lipophilic doxorubicin for breast cancer therapy. Int J Nanomedicine. 2019;14:4961-74. https://doi.org/10.2147/IJN.S209325.
16. Garg NK, Tyagi RK, Sharma G, Jain A, Singh B, Jain S, et al. Functionalized lipid-polymer hybrid nanoparticles mediated codelivery of methotrexate and aceclofenac: A synergistic effect in breast cancer with ımproved pharmacokinetics attributes. Mol Pharm. 2017;14(6):1883-97. https://doi.org/10.1021/acs.molpharmaceut.6b01148.
17. Liang J, Liu Y, Liu J, Li Z, Fan Q, Jiang Z, et al. Chitosan-functionalized lipid-polymer hybrid nanoparticles for oral delivery of silymarin and enhanced lipid-lowering effect in NAFLD. J Nanobiotechnol. 2018;16:64. https://doi.org/10.1186/s12951-018-0391-9.
18. Wang Q, Alshaker H, Böhler T, Srivats S, Chao Y, Cooper C, et al. Core shell lipid-polymer hybrid nanoparticles with combined docetaxel and molecular targeted therapy for the treatment of metastatic prostate cancer. Sci Rep. 2017;7:5901. https://doi.org/10.1038/s41598-017-06142-x.
19. Dave V, Tak K, Sohgaura A, Gupta A, Sadhu V, Reddy KR. Lipid-polymer hybrid nanoparticles: Synthesis strategies and biomedical applications. J Microbiol Methods. 2019;160:130-42. https://doi.org/10.1016/j.mimet.2019.03.017.
20. Shah S, Famta P, Raghuvanshi RS, Singh SB, Srivastava S. Lipid polymer hybrid nanocarriers: Insights into synthesis aspects, characterization, release mechanisms, surface functionalization and potential implications. Colloids Interface Sci Commun. 2022;46:100570. https://doi.org/10.1016/j.colcom.2021.100570
21. Hadinoto K, Sundaresan A, Cheow WS. Lipid-polymer hybrid nanoparticles as a new generation therapeutic delivery platform: a review. Eur J Pharm Biopharm. 2013;85(3 Pt A):427-43. https://doi.org/10.1016/j.ejpb.2013.07.002.
22. Singh A, Somvanshi P, Grover A. Pyrazinamide drug resistance in RpsA mutant (Δ438A) of *Mycobacterium tuberculosis*: Dynamics of essential motions and free-energy landscape analysis. J Cell Bio. 2019;120(5):7386-402. https://doi.org/10.1002/jcb.28013.
23. Zhang Y, Shi W, Zhang W, Mitchison D. Mechanisms of pyrazinamide action and resistance. Microbiol Spectr. 2014;2(4):MGM2-0023-2013. https://doi.org/10.1128/microbiolspec.MGM2-0023-2013.
24. Zimhony O, Cox JS, Welch JT, Vilchèze C, Jacobs WR Jr. Pyrazinamide inhibits the eukaryotic-like fatty acid synthetase I (FASI) of *Mycobacterium tuberculosis*. Nat Med. 2000;6(9):1043-7. https://doi.org/10.1038/79558.
25. Ramappa V, Aithal GP. Hepatotoxicity related to anti-tuberculosis drugs: Mechanisms and management. J Clin Exp Hepatol. 2013;3(1):37-49.https://doi.org/10.1016/j.jceh.2012.12.001.
26. Balay G, Abdella K, Kebede W, Tadesse M, Bonsa Z, Mekonnen M, et al. Resistance to pyrazinamide in *Mycobacterium tuberculosis* complex isolates from previously treated tuberculosis cases in Southwestern Oromia, Ethiopia. J Clin Tuberc Other Mycobact Dis. 2023;34:100411. https://doi.org/10.1016/j.jctube.2023.100411.
27. Singh A, Das SS, Ruokolainen J, Kesari KK, Singh SK. Biopolymer-capped pyrazinamide-loaded colloidosomes: *In-vitro* characterization and bioavailability studies. ACS Omega. 2023 Jul 7;8(28):25515-25524. https://doi.org/10.1021/acsomega.3c03135.

28. Eedara BB, Tucker IG, Das SC. Phospholipid-based pyrazinamide spray-dried inhalable powders for treating tuberculosis. Int J Pharm. 2016 Jun 15;506(1-2):174-83. https://doi.org/10.1016/j.ijpharm.2016.04.038.

29. Pham D, Fattal E, Tsapis N. Pyrazinamide-loaded poly(lactide-co-glycolide) nanoparticles: Optimization by experimental design. J Drug Deliv Sci Technol. 2015;30:384-390. https://doi.org/10.1016/j.jddst.2015.07.006.

30. Simões MF, Valente E, Gómez MJ, Anes E, Constantino L. Lipophilic pyrazinoic acid amide and ester prodrugs stability, activation and activity against M. tuberculosis. Eur J Pharm Sci. 2009;37(3-4):257-63. https://doi.org/10.1016/j.ejps.2009.02.012.

31. Salel S, Iyisan B. Polymer-lipid hybrid nanoparticles as potential lipophilic anticancer drug carriers. Discov Nano. 2023;18(1):114. https://doi.org/10.1186/s11671-023-03897-3.

32. Ebrahimian M, Mahvelati F, Malaekeh-Nikouei B, Hashemi E, Oroojalian F, Hashemi M. Bromelain loaded lipid-polymer hybrid nanoparticles for oral delivery: Formulation and characterization. Appl Biochem Biotechnol. 2022;194(8):3733-48. https://doi.org/10.1007/s12010-022-03812-z.

33. Hassan H, Adam SK, Alias E, Meor Mohd Affandi MMR, Shamsuddin AF, Basir R. Central composite design for formulation and optimization of solid lipid nanoparticles to enhance oral bioavailability of acyclovir. Molecules. 2021;26(18):5432. https://doi.org/10.3390/molecules26185432.

34. Parmar A, Kaur G, Kapil S, Sharma V, Sharma S. Central composite design-based optimization and fabrication of benzylisothiocynate-loaded PLGA nanoparticles for enhanced antimicrobial attributes. Appl Nanosci. 2020;10:379-89. https://doi.org/10.1007/s13204-019-01185-0.

35. Yu M, Yuan W, Li D, Schwendeman A, Schwendeman SP. Predicting drug release kinetics from nanocarriers inside dialysis bags. J Control Release. 2019;315:23-30. https://doi.org/10.1016/j.jconrel.2019.09.016.

36. Iftime MM, Dobreci DL, Irimiciuc SA, Agop M, Petrescu T, Doroftei B. A theoretical mathematical model for assessing diclofenac release from chitosan-based formulations. Drug Deliv. 2020;27(1):1125-33. https://doi.org/10.1080/10717544.2020.1797242.

37. Sheth P, Stein SW, Myrdal PB. Factors influencing aerodynamic particle size distribution of suspension pressurized metered dose inhalers. AAPS PharmSciTech. 2015;16(1):192-201. https://doi.org/ 10.1208/s12249-014-0210-z.

38. Debnath SK, Srinivasan S, Debnath M. Development of dry powder inhaler containing prothionamide-PLGA nanoparticles optimized through statistical design: *in-vivo* study. The Open Nanomedicine Journal. 2017;4(1):30-40. https://doi.org/10.2174/1875933501704010030.

39. Dai W, Zhang D, Duan C, Jia L, Wang Y, Feng F, et al. Preparation and characteristics of oridonin-loaded nanostructured lipid carriers as a controlled-release delivery system. J Microencapsul. 2010;27(3):234-41. https://doi.org/10.3109/02652040903079526.

40. Apostolou M, Assi S, Fatokun AA, Khan I. The effects of solid and liquid lipids on the physicochemical properties of nanostructured lipid carriers. J Pharm Sci. 2021;110(8):2859-2872. https://doi.org/10.1016/j.xphs.2021.04.012.

41. Xu L, Wang X, Yang G, Zhao Z, Weng Y, Li Y, Liu Y, Zhao C. Development of a concentration-controlled sequential nanoprecipitation for making lipid nanoparticles with high drug loading. Aggregate. 2023;4(6):e369. https://doi.org/10.1002/agt2.369.

42. Saharan P, Bhatt DC, Saharan SP, Bahmani K. The study the effect of polymer and surfactant concentration on characteristics of nanoparticle formulations. Der Pharm. Lett. 2015;7(12):365-371.

43. Nair AB, Sreeharsha N, Al-Dhubiab BE, Hiremath JG, Shinu P, Attimarad M, et al. HPMC- and PLGA-based nanoparticles for the mucoadhesive delivery of sitagliptin: Optimization and *in-vivo* evaluation in rats. Materials (Basel). 2019;12(24):4239. https://doi.org/10.3390/ma12244239.

44. Bohrey S, Chourasiya V, Pandey A. Polymeric nanoparticles containing diazepam: preparation, optimization, characterization, *in-vitro* drug release and release kinetic study. Nano Converg. 2016;3(1):3. https://doi.org/10.1186/s40580-016-0061-2.

45. Mirnezami SMS, Heydarinasab A, Akbarzadehkhyavi A, Adrjmand M. Development and optimization of lipid-polymer hybrid nanoparticles containing melphalan using central composite design and ıts effect on ovarian cancer cell lines. Iran J Pharm Res. 2021;20(4):213-228. https://doi.org/10.22037/ijpr.2021.114575.14923.

46. Tahir N, Madni A, Balasubramanian V, Rehman M, Correia A, Kashif PM, et al. Development and optimization of methotrexate-loaded lipid-polymer hybrid nanoparticles for controlled drug delivery applications. Int J Pharm. 2017;533(1):156-168. https://doi.org/10.1016/j.ijpharm.2017.09.061.

47. Gajbhiye KR, Salve R, Narwade M, Sheikh A, Kesharwani P, Gajbhiye V. Lipid polymer hybrid nanoparticles: a custom-tailored next-generation approach for cancer therapeutics. Mol Cancer. 2023;22(1):160. https://doi.org/10.1186/s12943-023-01849-0.

48. Sivadasan D, Sultan MH, Madkhali O, Almoshari Y, Thangavel N. Polymeric Lipid Hybrid Nanoparticles (PLNs) as emerging drug delivery platform-a comprehensive review of their properties, preparation methods, and therapeutic applications. Pharmaceutics. 2021;13(8):1291. https://doi.org/ 10.3390/pharmaceutics13081291.

49. Shafique M, Ur Rehman M, Kamal Z, Alzhrani RM, Alshehri

ISSN: 2458 - 8806

S, Alamri AH, et al. Formulation development of lipid polymer hybrid nanoparticles of doxorubicin and its *in-vitro, in-vivo* and computational evaluation. Front Pharmacol. 2023;14:1025013. https://doi.org/10.3389/fphar.2023.1025013.

50. Yadav P, Rastogi V, Verma A. Application of Box–Behnken design and desirability function in the development and optimization of self-nanoemulsifying drug delivery system for enhanced dissolution of ezetimibe. Futur J Pharm Sci. 2020;6:7. https://doi.org/10.1186/s43094-020-00023-3.
51. Saifullah B, Arulselvan P, Fakurazi S, Webster TJ, Bullo N, Hussein MZ, et al. Development of a novel anti-tuberculosis nanodelivery formulation using magnesium layered hydroxide as the nanocarrier and pyrazinamide as a model drug. Sci Rep. 2022;12(1):14086. https://doi.org/10.1038/s41598-022-15953-6.
52. Powder Flow, General Chapters: 1174, US Pharmacopoeia 29. [cited Feb 2025] Available from: http://www.pharmacopeia.cn/v29240/usp29nf24s0_c1174.html
53. Koduri SC, Napoleon AA. Mathematical model application for *in-vitro* release kinetics of ranolazine extended-release tablets. Dissol Technol. 2024;31(4):182-188.https://doi.org/10.14227/DT310424P182.
54. Fernández Tena A, Casan Clarà P. Deposition of inhaled particles in the lungs. Arch Bronconeumol. 2012;48(7):240-6. https://doi.org/10.1016/j.arbres.2012.02.003.
55. Paranjpe M, Müller-Goymann CC. Nanoparticle-mediated pulmonary drug delivery: A review. Int J Mol Sci. 2014;15(4):5852-73.https://doi.org/10.3390/ijms15045852.
56. Kole EB, Jadhav K, Sirsath N, Dudhe P. Nanotherapeutics for pulmonary drug delivery: An emerging approach to overcome respiratory diseases. J Drug Deliv Sci Technol. 2023; 81:104261. https://doi.org/10.1016/j.jddst.2023.104261.